# Feasibility study of spectral computed tomography (CT) with gold as a new contrast agent

Müllner M. a, Schlattl H. a, Oeh U. a, Hoeschen C. a, Dietrich O. b

<sup>a</sup> Helmholtz-Zentrum München, German Research Center for Environmental Health, Department of Medical Radiation Physics and Diagnostics, Ingolstädter Landstr. 1, 85764 Neuherberg, Germany;

b Josef Lissner Laboratory for Biomedical Imaging, Institute for Clinical Radiology, Ludwig-Maximilians-University Hospital Munich, Marchioninistr. 15, 81377 Munich, Germany

#### ABSTRACT

Newly developed spectral CTs with a photon-counting and energy-selective detector provide the possibility to obtain additional information about an object's absorption properties, the footprint of which can be found in the energy spectrum of the detected photons. These new CT systems are capable of yielding valuable insight into the elemental composition of the tissue and open up the way for new CT contrast agents by detecting element-specific K-edge patterns. Gold could be a promising new CT contrast agent. The major goal of this study is to determine the minimum amount of gold that is needed to use it as a spectral CT contrast agent for medical imaging in humans. To reach this goal, Monte Carlo simulations with EGSnrc were performed.

The energy-selective detector, on which this study is based, has 6 energy bins and the energy thresholds can be selected freely. First different energy thresholds were analyzed to determine the best energy thresholds with respect to detecting gold. The K-edge imaging algorithm was then applied to the simulation results with these energy bins. The reconstructed images were evaluated with respect to signal-to-noise ratio, contrast-to-noise ratio and contrast.

The K-edge imaging algorithm is able to convert the information in the six energy bins into three images, which correspond to the photoelectric effect, Compton scattering and gold content; however, it requires very long computing time. The simulations indicate that at least 0.2w% of gold are required to use it as a CT contrast agent in humans.

Keywords: Gold, contrast agent, spectral CT, Monte Carlo simulation, K-edge imaging

## 1. INTRODUCTION

Computed tomography (CT) is a common and widespread diagnostic tool in medical imaging. A normal X-ray source provides a polychromatic spectrum, but the standard charge-integrating CT detector just absorbs the incident photons and converts the number of photons to a single intensity value. This contributes to the problem that CT is not always able to distinguish between different materials. For example calcified cortical bone and tissue with a high amount of iodine contrast agent may have similar attenuation values. A possible solution for this problem would be the use of energy-resolving detectors. Newly developed spectral CTs (e.g. by Philips Healthcare, Hamburg, Germany) with a photon-counting and energy-selective detector provide the possibility to obtain additional information, which is graved in the energy spectrum of the transmitted photons. The new CT system is capable of yielding valuable insight into the elemental composition of the tissue and it opens up the way for new CT contrast agents by detecting element-specific K-edge patterns. The energy-selective detector developed by Philips has 6 energy bins; the energy thresholds can be selected freely and have a big impact on the results (figure 1).

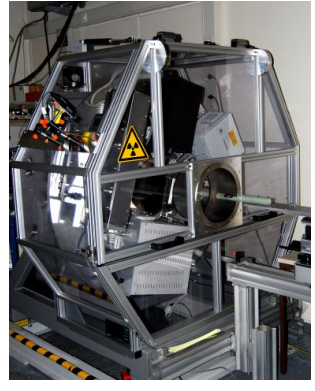
Gold could be a promising new CT contrast agent that can be easily coupled with biological targeting molecules (e.g. tumor-specific antibodies). By this coupling targeted tumor imaging should be possible. Furthermore the K-edge of gold is at 80.7keV, which lies well inside the diagnostic energy range.

Further author information: Send correspondence to Müllner M.

E-mail: marie.muellner@helmholtz-muenchen.de

Medical Imaging 2014: Physics of Medical Imaging, edited by Bruce R. Whiting, Christoph Hoeschen, Despina Kontos, Proc. of SPIE Vol. 9033, 90334A ⋅ © 2014 SPIE ⋅ CCC code: 1605-7422/14/\$18 ⋅ doi: 10.1117/12.2042988

The major goal of this study is to determine the minimum amount of gold required to use it as a spectral CT contrast agent for medical imaging in humans. At the outset of the investigation different energy thresholds for the bins of the energy-selective detector were analyzed to determine the best energy thresholds with respect to the detection of gold. The K-edge imaging algorithm was then applied to the simulation results.



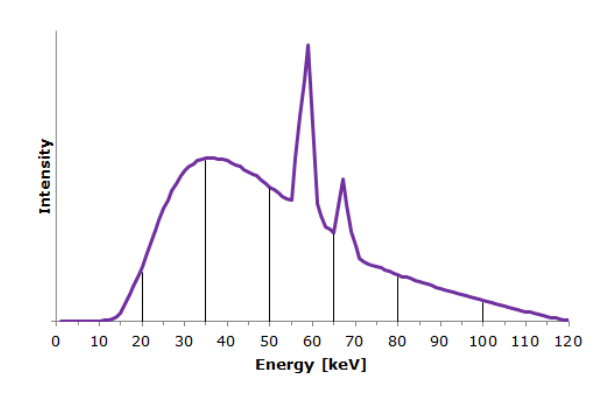


Figure 1. Philips prototype small animal spectral CT (left) and polychromatic X-ray spectrum (120kV) with 6 energy bins (right).

## 2. MONTE CARLO SIMULATIONS

## 2.1 Simulations with EGSnrc

Spectral CT images were simulated with the Monte Carlo simulation code EGSnrc, which simulates the coupled transport of electrons and photons. Transport of charged particles is simulated with the condensed history technique. Cross sections for the photoelectric effect, Rayleigh scattering and pair production are in agreement with the XCOM/NIST database. For the imaging simulations the cutoff energy for photons was 1 keV and for electrons 60 keV. The particles energy is locally deposited, if it is below the cutoff energy.

Two different voxel phantoms were used for the simulations. The purpose of the first voxel phantom was to determine the minimum amount of gold that is needed to use it as a CT contrast agent in humans and to investigate the influence of different sizes of region of interests (ROI).

The diameter of the simple voxel phantom is 30 cm and it consists of simulated liver parenchym ( $\rho = 1.06 \text{g/cm}^3$ ) and five sets of four of metastases ( $\rho = 1.02 \text{g/cm}^3$ ). The metastases have a size of  $1.4 \times 1.4 \text{ cm}^2$ ,  $1.05 \times 1.05 \text{ cm}^2$ ,  $0.7 \times 0.7 \text{ cm}^2$  and  $0.35 \times 0.35 \text{ cm}^2$ . For each set of metastases a different amount of gold (0.7 w%, 0.4 w%, 0.3 w%, 0.2 w% and 0.1 w%) is added to the metastases (figure 2(a)).

The results from the simple voxel phantom are then used for the human voxel phantom, which is based on CT data of a real female.<sup>2</sup> The purpose of this second phantom is to investigate the effect of gold as a contrast agent in small tumors or metastases in the liver. The three metastases are implemented in the voxel phantom and have a size of  $1.24 \times 1.24$  cm<sup>2</sup>,  $0.88 \times 0.88$  cm<sup>2</sup> and  $0.35 \times 0.35$  cm<sup>2</sup>. The chemical composition of the organs is based on the ICRU report 44.3 The CT slice used for the simulations is shown in figure 2(b). For all simulations, the focus detector distance (FDD) is 104 cm and the focus object distance (FOD) is 57 cm. 1160 views are performed and the number of histories per view is  $10^9$ . The slice thickness is 1.6 mm. For the simple voxel phantom the detector has 580 detector elements, each with a size of 1.5 mm. For the human voxel phantom the detector has 640 detector elements, each with a size of 1.6 mm. An ideal detector is implemented, i.e. all incident photons are detected, the count rate is unlimited and the energy resolution is perfect.

# 2.2 Optimizing the bin thresholds

The bins just below the K-edge of gold and just above the K-edge are very important for the efficient detection of gold. The incoming photons are stored in arrays corresponding to the photon energy (in steps of 1keV). To analyze the effect of different bin sizes above and below the K-edge of gold, the array elements are summed up

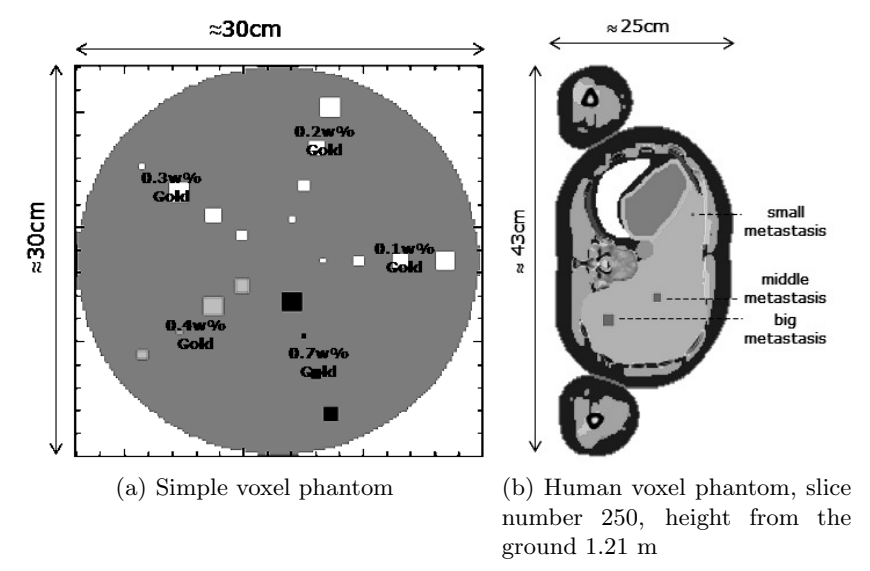


Figure 2. Voxel phantoms used for the Monte Carlo simulations

and the CT images are then reconstructed. To investigate to optimal width of the two energy bins just below and above the K-edge of gold, the signal-difference-to-noise ratio (SDNR) criterion is used:<sup>4</sup>

$$SDNR = \frac{\overline{\mu}_{CTabove} - \overline{\mu}_{CTbelow}}{\sqrt{\sigma_{CTabove}^2 + \sigma_{CTbelow}^2}}$$
(1)

with  $\overline{\mu}_{\text{CTabove}}$  and  $\overline{\mu}_{\text{CTbelow}}$  being the average linear attenuation coefficient and  $\sigma_{\text{CTabove}}^2$  and  $\sigma_{\text{CTbelow}}^2$  describe the variance in the ROI in the reconstructed CT images in the bin above and below the K-edge. Equation 1 needs to be maximized under the constrained

$$\overline{\mu}_{\text{XCOMabove}} > \overline{\mu}_{\text{XCOMbelow}}$$
 (2)

 $\overline{\mu}_{\text{XCOMabove}}$  and  $\overline{\mu}_{\text{XCOMbelow}}$  are the linear attenuation coefficients (calculated with XCOM) in the bin below and above the K-edge of gold.

# 2.3 K-edge decomposition algorithm

The basic idea of the K-edge decomposition algorithm is to calculate the fractional contribution to the total attenuation of the photoelectric effect, Compton scattering and the high-Z material (in our case gold). Since the contribution of various physical processes to the photon absorption is energy dependent, their proportions to the reconstructed image (i.e. the absorption coefficients  $\mu$ ) are different in each energy bin. By a decomposition technique, also called K-edge imaging,<sup>5,6</sup> this energy dependent attenuation information is exploited. For the present study, the attenuation is assumed to be composed of the cross sections of the photoelectric effect, Compton scattering and a term, which corresponds to gold, thus

$$\mu(E, \vec{x}) = a_{\text{photo}}(\vec{x}) \frac{1}{E^3} + a_{\text{compton}}(\vec{x}) f_{\text{KN}} \left(\frac{E}{E_e}\right) + a_{\text{gold}}(\vec{x}) f_{\text{gold}}(E)$$
(3)

where E is the energy,  $E_e \approx 511 \mathrm{keV}$  is the rest mass energy of the electron and the space dependence of the attenuation is described by  $\vec{x}$ .  $f_{\mathrm{KN}}$  describes the Compton cross section and is represented by the Klein-Nishina function and  $f_{\mathrm{gold}}$  is the energy dependent mass attenuation coefficient of gold. The decomposition algorithm solves for the unknown coefficients  $a_{\mathrm{photo}}$ ,  $a_{\mathrm{compton}}$  and  $a_{\mathrm{gold}}$ , with  $a_{\mathrm{gold}}$  being the density of gold in the tissue. Compton scattering is independent of the atomic number Z of the material, the Compton image will therefore provide low contrast information, i.e., it is more sensitive to soft tissue contrast. The photoelectric absorption

is proportional to Z<sup>4</sup>, and thus the photoelectric image will mainly provide information about materials with a high atomic number (except the contrast agent, since that information is in the third parameter  $a_{\rm gold}$ ), e.g.

The evaluation of the image quality is done with respect to the signal-to-noise ratio (SNR), the contrast-to-noise ratio (CNR) and the contrast in the reconstructed images. A bilateral filter algorithms, implemented by O. Tischenko (private communication), is applied to further enhance the images and suppress noise. The SNR is defined as the ratio of the mean value in the region of interest  $\overline{\mu}_{ROI}$  and the standard deviation  $\sqrt{\sigma_{ROI}^2}$ 

$$SNR_{CT} = \frac{\overline{\mu}_{ROI}}{\sqrt{\sigma_{ROI}^2}} \tag{4}$$

The CNR takes into account the signal and noise features of the reconstructed images. The CNR is defined as the ratio of the contrast between the ROI  $\overline{\mu}_{ROI}$  and the background  $\overline{\mu}_{B}$  and the noise.<sup>7</sup>

$$CNR = \frac{|\overline{\mu}_{ROI} - \overline{\mu}_B|}{\sqrt{\sigma_{ROI}^2 + \sigma_B^2}}$$
 (5)

where  $\sigma_{\mathrm{ROI}}^2$ ,  $\sigma_B^2$  are the variances respectively.

The contrast is defined as<sup>8</sup>

$$C = \frac{|\overline{\mu}_{ROI} - \overline{\mu}_B|}{\overline{\mu}_{ROI} + \overline{\mu}_B}$$
 (6)

## 3. RESULTS AND DISCUSSION

As a first step the optimal bin thresholds for the bin below and above the K-edge of gold were calculated with respect to the SDNR. The results, i.e. the bins with the maximum SDNR, are summarized in tables 1, 2 and 3.

Table 1. Comparison of the SDNR for the simple voxel phantom.

	0.7w% Gold	0.4w% Gold	0.3w% Gold	0.2w% Gold	0.1w% Gold
below K-edge	[74,81)  keV	[73,81)  keV	[77,81)  keV	[77,81)  keV	[78,81)  keV
above K-edge	[81,84)  keV	[81,86)  keV	[81,86)  keV	[81,85)  keV	[81,83)  keV
SDNR	2.2303	1.7582	1.4776	0.98676	0.39692

Table 2. Comparison of the SDNR for the human voxel phantom with 0.3w% gold.

	big metastasis	middle metastasis	small metastasis
below K-edge	[75,81)  keV	[77,81)  keV	[75,81) keV
above K-edge	[81,86) keV	[81,86)  keV	[81,85) keV
SDNR	1.1726	1.7384	1.6755

For the following investigations the bin thresholds below the K-edge were set to [75,81) keV and the bin thresholds

Table 3. Comparison of the SDNR for the human voxel phantom with 0.2w% gold.

	big metastasis	middle metastasis	small metastasis
below K-edge	[75,81)  keV	[77,81)  keV	[75,81)  keV
above K-edge	[81,86) keV	[81,86)  keV	[81,85)  keV
SDNR	0.66802	1.0751	1.0198

above the K-edge were set to [81,86) keV. The intensity of the X-ray spectrum above 86 keV is low, that means only a small number of photons is generated. In order to produce as little as possible noise in this bin, the bin thresholds were set to [86,120] keV. For the remaining three bins the intensity  $I(E,\eta) = I_0(E) \exp(-\mu_{\text{Bone}}(E)\eta)$ was calculated for different bin thresholds. It was assumed that X-rays are traveling a constant distance  $\eta=30$  cm. The linear attenuation coefficient  $\mu_{\text{Bone}}(E)$  was calculated with XCOM. The goal was to have a high difference in these intensities for each of the three bins. The first bin was set to [25,47) keV, as  $I(E,\eta)$  is almost equal to zero, if the upper threshold is below 47 keV. The bin thresholds for the third bin were set to [60,75) keV, due to the fact, that  $I(E,\eta)$  has a maximum for these bin thresholds. The thresholds for the remaining second bin were [47,60) keV. (These new bin thresholds are referred to as optimized bin thresholds). As a reference the energy thresholds introduced by Cormode et al.<sup>9</sup> were used: [25,34), [34,51), [51,80), [80,91), [91,110) and [110,120] keV (referred to as non-optimized bin thresholds). It was stated that these energy thresholds, provided the highest sensitivity with regard to simultaneous imaging of iodine and gold. The energy thresholds for the non-optimized and optimized case are shown in figure 3.

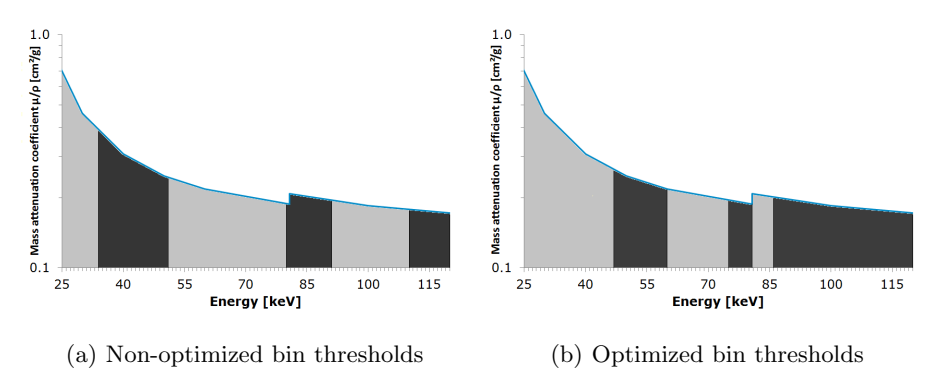


Figure 3. Mass attenuation curve of 0.2w% gold with the different bin thresholds for the optimized and non-optimized case.

The different performance results of the K-edge decomposition algorithm are shown in figure 4. The K-edge decomposition algorithm performs much better for the optimized bin thresholds than for the non-optimized bin thresholds. In the Compton effect images (figure 4(b) and (f)) the metastases with 0.7w%, 0.4w% and 0.3w% gold are still visible, the metastases with 0.2w% and 0.1w% gold are not visible. The K-edge decomposition algorithm seems to overestimate the compton effect. The positive contributions from 0.7w%, 0.4w% and 0.3w% gold in the compton effect image lead to the assumption that the K-edge decomposition does not work optimally for higher gold amounts. In the photoelectric image (figure 4(e)) gold is clearly removed and there are "holes" in the image. The strong noise in the photoelectric images is partly due to the absence of materials with a high atomic number. The probability of the photo effect at the used energies is therefore very low leading to high noise. The gold images (figure 4(c) and (g)) are very noisy. The minimal amount of gold which is clearly visible in the simple voxel phantom (optimized bin thresholds) is 0.2w%. For the metastases with 0.1w% gold a clear distinction between signal and noise is not possible. For 0.3, 0.4 and 0.7w% even the smallest metastases are clearly identifiable. These simulations indicate that at least 0.2w% gold are needed to use it as a CT contrast agent in humans. Even the small metastases with a size below 1 cm<sup>2</sup> can be detected. For the human voxel phantom only the results for the optimized bin thresholds are shown. The results of the K-edge decomposition algorithm for the human voxel phantom with 0.3w% and 0.2w% gold are shown in figure 5. The photoelectric images (figure 5(a) and (e)) mainly show bones. The Compton scattering images (figure 5(b) and (f)) provide good soft tissue contrast. As expected, no gold is visible in the photoelectric and Compton scattering images. All three metastases with 0.3w% are clearly recognizable in the unfiltered and the filtered images (figure 5(c) and (d)). For the metastases with 0.2w% gold it is harder to distinguish between noise and signal in the gold image (figure 5(g) and (h)). Nevertheless, all three metastases are still identifiable.

The SNR and the CNR of the filtered images is significantly higher than for the unfiltered images for all simulations. For the simple voxel phantom the contrast slightly increases after filtering the image, but for the human voxel phantom the contrast slightly decreases after filtering (table 4). The high noise level in the gold images induce significantly smaller SNR, CNR in the gold images than for the standard CT image with an energy-integrating detector. However the contrast is much higher in the gold images compared to the standard CT image.

The numerical values in the gold images should represent the fractional weight of gold in the tissue. The values are summarized in table 5. Without any processing of the gold images the algorithm overestimates the amount of gold by a factor of around 1.5 for the 0.7w% gold up to a factor of 2.75 (simple voxel phantom) and 2.45

## Non-optimized bin thresholds

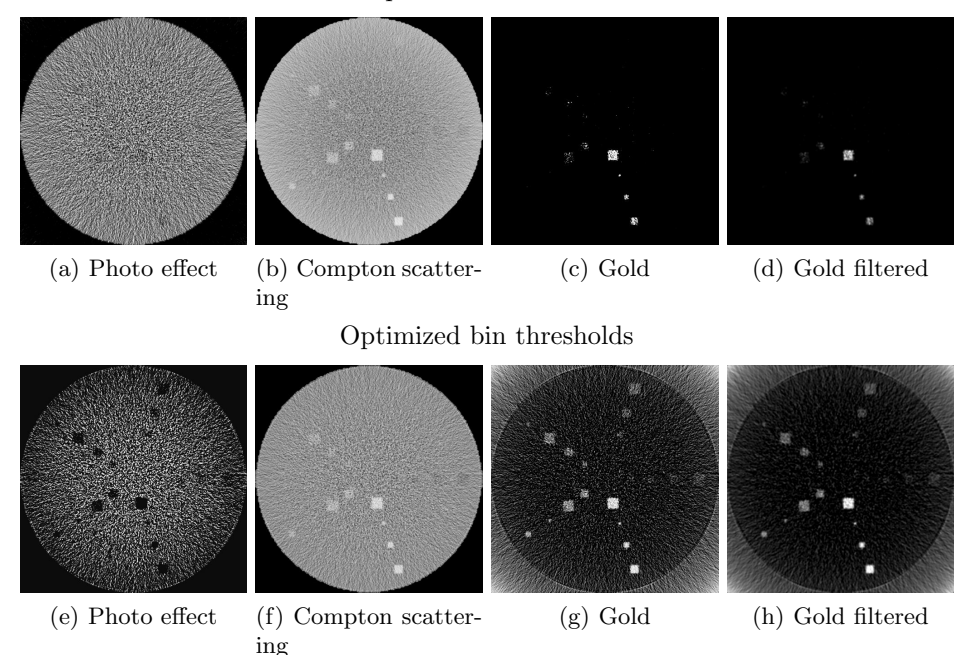


Figure 4. Results of the K-edge decomposition algorithm for the simple voxel phantom for the non-optimized and optimized bin thresholds.

(human voxel phantom) for 0.2w% gold. The smaller the amount of gold, the higher is the overestimation. As can be seen in the gold images (figure 4(g), 5(c) and (g)) the noise in the region without gold is high, i.e., the numerical background values are not equal to zero. Subtraction of the mean numerical background value yield the values in the last row of table 5. These values are close to the implemented fractional weights of gold.

Table 4. Performance results of the K-edge decomposition algorithm for the unfiltered and filtered optimized gold images. As comparison the SNR, CNR and contrast for the standard CT image with an energy-integrating detector is given.

	simple voxel phantom			human voxel phantom, 0.3w% gold			human voxel phantom, 0.2w% gold		
	SNR	CNR	C	SNR	CNR	C	SNR	CNR	C
unfiltered	3.824	1.816	0.4543	2.806	1.195	0.4255	2.757	0.7939	0.2889
filtered	7.023	3.658	0.4911	8.176	3.643	0.4161	8.431	2.5431	0.2781
energy-integrating	75.13	5.009	0.0574	91.30	5.049	0.0366	93.02	2.5710	0.0181
detector									

Table 5. Implemented and calculated amounts of gold for the K-edge decomposition algorithm.

						human voxel	
	simple voxel phantom			phantom			
implemented [w%]		0.4	0.3	0.2	0.1	0.3	0.2
calculated [w%] (with background)		0.71	0.62	0.55	0.43	0.53	0.49
calculated [w%] (minus background)	0.80	0.43	0.34	0.28	0.15	0.32	0.22

## 4. CONCLUSION

Gold is a promising new CT contrast agent. The big advantage of spectral CT is the possibility to better differentiate between different tissues and to specifically detect gold. The K-edge imaging algorithm is able to convert the information in the six energy bins into three images, which correspond to the contribution of the

Human voxel phantom with 0.3w% gold

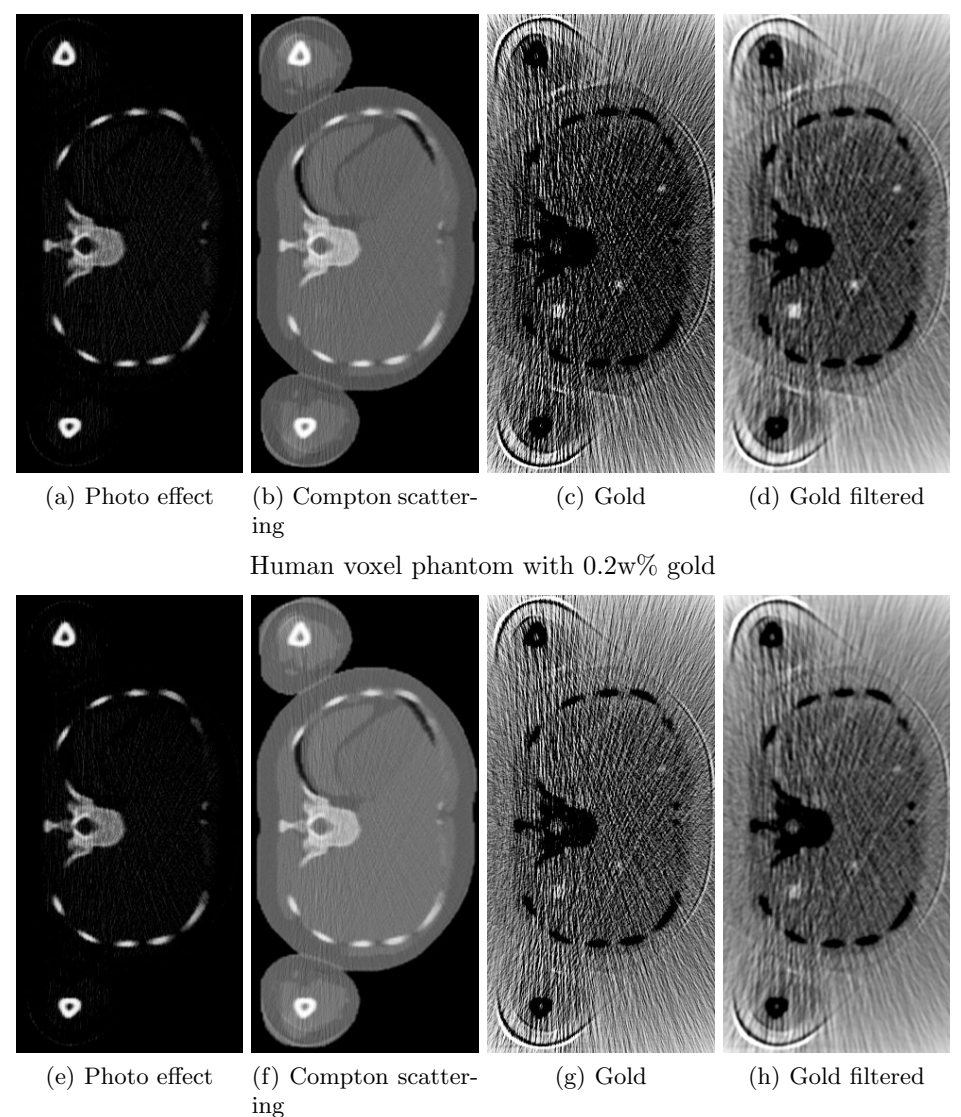


Figure 5. Results of the K-edge decomposition algorithm for the human voxel phantom with  $0.3\mathrm{w}\%$  and  $0.2\mathrm{w}\%$  gold.

photoelectric effect, Compton scattering and gold.

The accomplished results provide a lower limit of 0.2w% on the required gold enrichment in malignant tissue for improved cancer detection. It remains to be examined whether and how this can be achieved in practice. Besides K-edge imaging, several advanced imaging methods can potentially be realized with spectral CT and it still needs to be examined, which method is the most suitable for gold enhanced medical imaging in humans.

## REFERENCES

- [1] Steidley, J. W., "Exploring the spectrum Advances and potential of spectral CT," (2008). http://clinical.netforum.healthcare.philips.com/us\_en/Explore/White-Papers/CT/Exploring-the-spectrum-Advances-and-potential-of-spectral-CT.
- [2] Taranenko, V., Zankl, M., and Schlattl, H., "Voxel phantom setup in MCNPX," in [American Nuclear Society Topical Meeting in Monte Carlo, Chattanooga, TN], (2005).
- [3] Bethesda, M., "Report 44 of the International Commission on Radiation Units and Measurements," tech. rep., Tissue Substitutes in Radiation Dosimetry and Measurement (1989).

- [4] He, P., Wei, B., Cong, W., and Wang, G., "Optimization of K-edge imaging with spectral CT.," *Med Phys* **39**, 6572–6579 (Nov 2012).
- [5] Roessl, E. and Proksa, R., "K-edge imaging in x-ray computed tomography using multi-bin photon counting detectors.," *Phys Med Biol* **52**, 4679–4696 (Aug 2007).
- [6] Schlomka, J. P., Roessl, E., Dorscheid, R., Dill, S., Martens, G., Istel, T., Bumer, C., Herrmann, C., Steadman, R., Zeitler, G., Livne, A., and Proksa, R., "Experimental feasibility of multi-energy photon-counting K-edge imaging in pre-clinical computed tomography.," *Phys Med Biol* 53, 4031–4047 (Aug 2008).
- [7] Shikhaliev, P. M., "The upper limits of the SNR in radiography and CT with polyenergetic x-rays.," *Phys Med Biol* **55**, 5317–5339 (Sep 2010).
- [8] Shikhaliev, P. M., "Photon counting spectral CT: improved material decomposition with K-edge-filtered x-rays.," *Phys Med Biol* **57**, 1595–1615 (Mar 2012).
- [9] Cormode, D. P., Roessl, E., Thran, A., Skajaa, T., Gordon, R. E., Schlomka, J.-P., Fuster, V., Fisher, E. A., Mulder, W. J. M., Proksa, R., and Fayad, Z. A., "Atherosclerotic plaque composition: analysis with multicolor CT and targeted gold nanoparticles.," *Radiology* 256, 774–782 (Sep 2010).